# Synthesis and Characterization of Novel Multifunctional $SiO_2$ Nanoparticles

*Ayşe Aslan*[a], Ali Murat Soydan[b], Ayhan Bozkurt[c]*

[a]Gebze Technical University, Department of Bioengineering, Cayirova 41400 Gebze/Kocaeli
[b]Gebze Technical University, Department of Materials Science and Engineering, Cayirova 41400 Gebze/Kocaeli
[c]Fatih University, Department of Chemistry, 34500 Büyükçekmece İstanbul / Turkey

**Abstract**
In this study, the synthesis and characterization of multifunctionalized silica nanoparticles for biomedical applications were clarified. For the preparation of azole functional $SiO_2$, a two-step method based on hydrolyzed of TEOS was used in this study. The epoxy functional $SiO_2$ nanoparticles modified with 5-Amino-Tetrazole (ATet-$SiO_2$), in order to obtain 1,2,4- 5-Amino-Tetrazole functional $SiO_2$ molecules via ring opening of the epoxy ring. FT-IR, SEM, TEM and AFM analysis were confirmed the functionalization of $SiO_2$. TGA and DSC were employed to examine the thermal stability and homogeneity of the materials. The thermal and proton conducting property of material was investigated under anhydrous state. TGA showed that the samples are thermally stable up to approximately 250$^o$C. anticancer effects of Aminotetrazole was investigated at concentrations (10, 50, 100, 500, 1000, 5000µg/ml) on Hela cells during 72h exposure using the xCELLigence system. Our data suggests that the xCELLigence live cell analysis system offers dynamic to use ATet-$SiO_2$, as an alternative anticancer drug. The xCELLigence system can be used as a rapid monitoring tool for cellular viability and be applied in anticancer testing of chemical substances using in vitro cell cultures.

**Keywords:** Biomaterials; Morphological Analysis; Nanomaterials; Conducting properties; Anticancer

## 1. Introduction

The advent of nanoparticles new avenues in many different fields of studies along with other nanomaterials via smaller size and high surface to volume ratio of nanoparticles are the key features which make them useful in the biomedical fields because of the development of many new properties, ease of functionalization, conjugation of biomolecules etc. [1-4]. The application of nanotechnology has been the development and use of multifunctional nanoparticles, which can be used to map cellular components and monitor and track them in real time and as drug delivery vehicles or therapeutic agents [5-7].

Multifunctionalized nanoparticles are emerging as ideal tools for gene/drug delivery, bioimaging, labeling, or intracellular tracking in biomedical applications, and have attracted considerable attention owing to their unique advantages [8-10].

Several methods are used to functionalize silica nanoparticles; we report yet another original and effective method for generating (epoxied) nanoparticles with a high surface concentration of epoxy functionalities. The method is developed as a pathway for generation of functional silica with different molecules for diverse applications. Specifically, a proven method of permanent surface modification of organic surfaces with azole containing molecules groups were transferred to the epoxy modification nanoparticles.

## 2. Experimental

The intention of the present work was to develop an alternative method for the synthesis of modified silica nanoparticles starting from fundamental molecules instead of using already synthesized silica nanoparticles. For this purpose, TEOS which has been the starting molecule for the synthesis of silica nanoparticles in Stöber reaction [11-13].The resultant particles were collected with a membrane filter and washed with water and ethanol several times.

**a)**

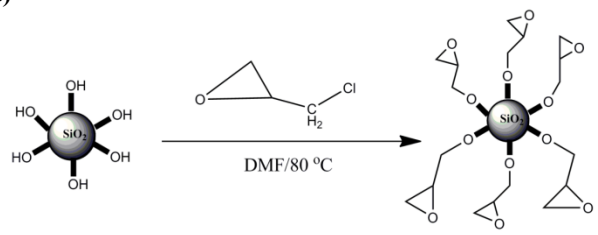


**b)**

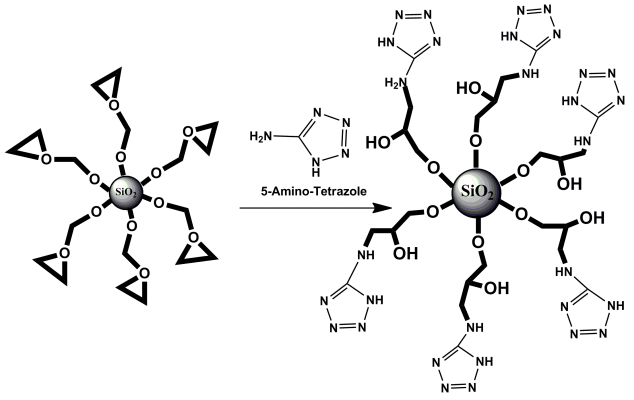


**Figure 1. a)** Synthesis of the epoxy modified $SiO_2$ nanoparticles **b)**Synthesis of the 5-Amino-Tetrazole functional $SiO_2$ nanoparticles (ATet- $SiO_2$).

$SiO_2$ was dispersed in THF and epichlorohydrin was added to solution. When the reaction occurred between epichlorohydrin and surface of silica, the HCl gas released. The modification ratio with epichloroydrin calculated by back titration method of releasing of HCl, was bubbled to NaOH solution. The temperature was set to 80$^{o}$C (see Figure 1a). The modified silica nanoparticles were obtained after precipitation and washed with water/methanol solution several times. Then, it was filtered and dried at 80 $^{o}$C under vacuum.

In order to prepare 5-Amino-Tetrazole functional $SiO_2$ (see Figure 1), the modified silica was dissolved in DMF and stoichiometric amounts of 5-Amino-Tetrazol were added to the solution. The temperature was set to 100 $^{0}$C and the mixture was stirred under nitrogen atmosphere for 24 hours. The resulting solid mixture was filtered and dialyzed against water to remove excess 5-Amino-Tetrazole.

## 3. Characterizations and Results

### 3.1. FT-IR

FT-IR spectra of azole functional $SiO_2$ is represented in Fig. 2. The absorption peaks at 1132 cm$^{-1}$ and 1045 cm$^{-1}$ attributed to Si–O–Si asymmetric stretching. The peak at 3435 cm$^{-1}$ belonged to Si–OH stretching vibration. A distinctive C=C stretching was displayed at about 1603 cm$^{-1}$. The following bands are well established to specific molecular motions that can be taken as the silica fingerprint [14-16]. The signals at 1220 and 1083 cm$^{-1}$ belong to Si–O stretching. The band centered at 954 cm$^{-1}$ is associated with the stretching mode of non-bridging oxide bands as Si–OH and Si–O. The band around at 795 cm$^{-1}$ is assigned to the symmetric stretching of the Si–O–Si mode. The lowest frequency modes (550 and 470 cm$^{-1}$) are associated with the rocking motions perpendicular to the Si–O–Si plane, of the oxygen bridging two adjacent Si atoms that formed the tetra or trisiloxane rings [15,17].

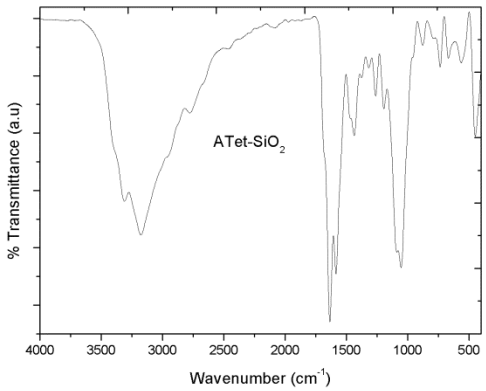


**Figure 2.** FT-IR spectra of the ATet-$SiO_2$ nanoparticle

The absorption at 900 cm$^{-1}$ is assigned to stretching vibration of the epoxy group which moved out on azole functionalization[18,19]. Azole functional $SiO_2$ exhibited a medium absorption at 1577 cm$^{-1}$ and 1450 cm$^{-1}$ due to C=N and C-N stretching of the triazole ring [20]. The bands below 1800 cm$^{-1}$ are attributed to chains and ring skeletal vibrations of H–C–H, C O, H–N–H, C–N. The strong signal at 1630cm$^{-1}$ is related to an in-plane deformation mode of $NH_2$ group, and the ones at 1604 and 1571 cm$^{-1}$ to N–H vibration in plane and C O stretching. The series of five fairly strong absorptions between 1500 and 1300 cm$^{-1}$ assigned to ring vibrations C-N single and double bonds, and also to a deformation mode of CH groups.

### 3.2XRD

The X-ray diffractograms of functional silica nanoparticles showed the wide peak with the highest intensity centered at 22$^{\circ}$ (2Θ), assigned to the characteristic reflection of amorphous silica. The average crystallite diameter (L) was estimated by Scherrer's equation

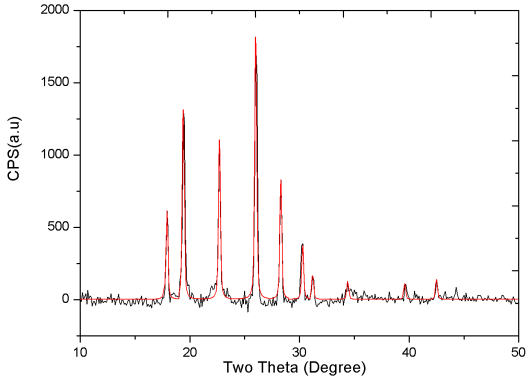


Figure 3. XRD patterns of Azole functional $SiO_2$.

The intense diffraction peak at 2θ = 25° was significantly weakened as seen at Fig. 3b. When ATet functional silica nanoparticles were incorporated into $SiO_2$ the peak at 25° becomes more shaper because of the superimposition of peaks of 5-Amino-Tetrazole and nanoparticles [21]. The result shows that the particle size of ATet-$SiO_2$ was calculated as 45±3 nm. The XRD data of the materials indicated that the surface of silica nanoparticles functionalized with azole units the size of particles increasing with azole units and the peak of characteristic reflection peak of amorphous silica was slightly shifted.

### 3.3 Morphology

The modification on the surface of $SiO_2$ is clearly seen in Fig. 4. Here a pronounced difference is seen when comparing the epoxy functional and the azole modified particles.

a) b)

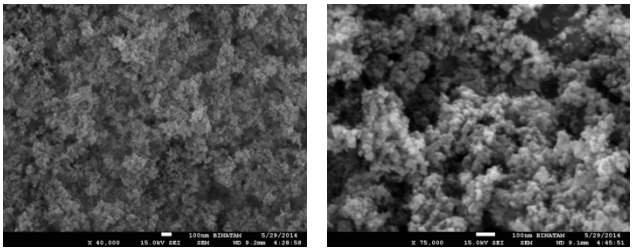

**Figure 4.** SEM micrographs of the azole functional materials a) Epoxy modified $SiO_2$ b) ATri-$SiO_2$ c) ATet-$SiO_2$

After modification of silica nanoparticles with azole molecules via ring opening reaction of epoxy, SEM images such as that in Figure 4a show the formation of epoxidation on the approximately 12 nm diameter $SiO_2$ particles. The particle diameter in XRD result ATet-$SiO_2$ is ~45 nm after modification with tetrazole units, indicating a ~30 nm thick layer on the $SiO_2$.

### 3. 4Thermal analysis

The melting temperature, $T_m$ of ATet-$SiO_2$ functional material was measured. Incorporation of ATet-$SiO_2$ with pure ATet would fill the free volumes and would cause need to more energy for starting motions, which would make Tm to increase. Table 1 shows the Tm of ATet functional samples under inert atmosphere at a scan rate of 10 $^oC$ $min^{-1}$. The melting points of Amino-tetrazole functional $SiO_2$ (ATet-$SiO_2$) is 162 $^oC$. After functionalization on $SiO_2$ surface the Tm of the azole units shifted to higher temperature.

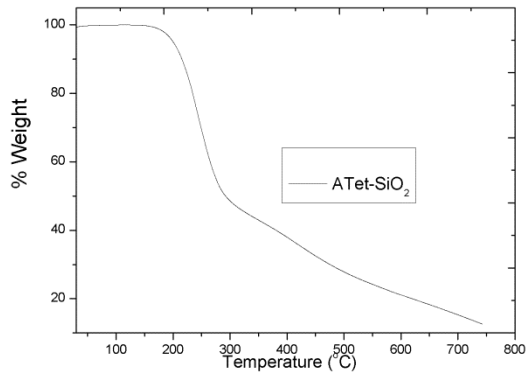


**Figure 5.** TG thermograms of Azole functional $SiO_2$ recorded at a heating rate of 10 $^oC$/min under a nitrogen atmosphere.

Figure 5.shows the thermogram of ATet-$SiO_2$ plot of weight loss versus temperature provide an estimate of the quantity of azole units from the nanoparticles. The functional particles consist of both thermally stable compounds that remain in the residue (silica bound to the azole units) and decomposable brushes and initiators that contribute to weight loss. After functionalization from the particle, TGA shows a total weight loss of 90%, which corresponds to azole functionalization ratio, is approximately 90%. Reaction of azole functionalization leads to a total weight loss of approximately 90%, which is consistent with essentially complete functionalization between azole units and silica nano particles. After 250$^oC$ a remarkable weight loss derives from the thermal decomposition of the azole units

.

### 3.5 Anticancer Effect Results

The xCELLigence system allowed the comparison of the cytotoxic effect of these concentrations which were selected for subsequent studies. The cytotoxicity of ATet-$SiO_2$ was observed using this method was slightly lower than that obtained using the end-point MTT assay. For the first 24 h, the number of Hela cells grew in almost direct proportion to the time of culture. The replacement of the old medium with a fresh one caused a slight decrease in CI(cell index) of control cells, which was probably related to stress. One hour later, the value of CI started increasing, which continued until the end of the experiment. The addition of each dose of, ATet-$SiO_2$ resulted in an abrupt decrease in impedance and only cells treated with the 10, 50, 100, 5000µg/ml concentrations of ATet-$SiO_2$ .

In figure 6 presented that after 24 hour addition of ATet-$SiO_2$ at concentration 10,50,100 and 5000 µg/ml are more effective on HeLA cell to decrease cell ındex.

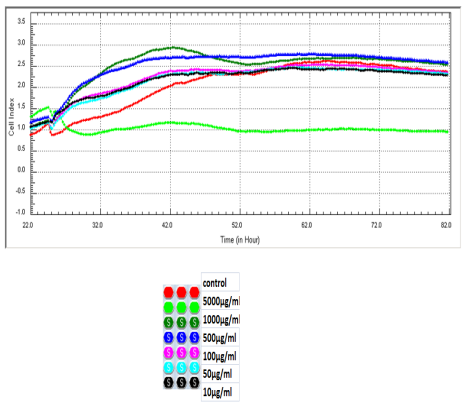


**Figure 6.** Results of the xCELLigence system treated with different concentration of ATet-$SiO_2$ on Hela cells.

### 3.6 Proton conductivity

The alternating current (AC) conductivity, $\sigma_{ac}$ (ω) of the material was measured at several temperatures using impedance spectroscopy. The proton conductivity of anhydrous sample was measured from 20 $^{o}$C to 150 $^{o}$C. Among the azole functional $SiO_2$ materials ATri-$SiO_2$ showed the highest proton conductivity of 0.006 $Scm^{-1}$ at 150 $^{o}$C under anhydrous conditions.

### 4.Conclusions

The azole functional silica nanoparticles have been synthesized via two-step methods. Silica was synthesized with Scthöber method of TEOS and functionalized with azole units on silica surface. Azole units were immobilized by ring opening of the epoxide ring. The back titration method was used for determined of functionalization ratio. The functionalization ratio was calculated above 90%. The structures of the azole functional silica were proved by FT-IR. XRD and SEM results illustrated the functionalization of the $SiO_2$ also the diameter of the $SiO_2$ nanoparticles increasing with azole modification up to approximately 45 nm. Anhydrous proton conducting properties and thermal properties functional materials were investigated. The TGA thermograms showed that the materials are thermally stable up to 250 $^{o}$C. The proton conductivity of the ATet-$SiO_2$ increased with the temperature. ATet-$SiO_2$ showed a maximum water-free proton conductivity of approximately, 0.006 $Scm^{-1}$ at 150 $^{0}$C. Azole functional $SiO_2$composites can be suggested as proton conducting solid materials for application in high temperature (PEMFC). As an updated research of the good representative azole modified silica nanoparticles may lead to programmed cell death via cytotoxic pathways on HeLa cell line. Azole functional $SiO_2$ different concentrations has anti-proliferative effects on HeLa cell line. Also, this study has the unique feature of being studied with Azole functional $SiO_2$ material.

### 5. References

(1) Wang, L.; Zhao, W. J.; Tan, W. H. *Nano Res* **2008**, *1*, 99.

(2) Li, Z.-Z.; Xu, S.-A.; Wen, L.-X.; Liu, F.; Liu, A.-Q.; Wang, Q.; Sun, H.-Y.; Yu, W.; Chen, J.-F. *Journal of Controlled Release* **2006**, *111*, 81.

(3) Niemeyer, C. M. *Angewandte Chemie International Edition* **2001**, *40*, 4128.

(4) Salata, O. *Journal of nanobiotechnology* **2004**, *2*, 3.

(5) Trewyn, B. G.; Giri, S.; Slowing, II; Lin, V. S. *Chem Commun (Camb)* **2007**, 3236.

(6) Ow, H.; Larson, D. R.; Srivastava, M.; Baird, B. A.; Webb, W. W.; Wiesner, U. *Nano letters* **2005**, *5*, 113.

(7) Ye, Z. Q.; Tan, M. Q.; Wang, G. L.; Yuan, J. L. *Journal of Materials Chemistry* **2004**, *14*, 851.

(8) Jin, S.; Ye, K. M. *Biotechnol Progr* **2007**, *23*, 32.

(9) Rosenholm, J. M.; Sahlgren, C.; Linden, M. *Nanoscale* **2010**, *2*, 1870.

(10) Lai, C. Y.; Trewyn, B. G.; Jeftinija, D. M.; Jeftinija, K.; Xu, S.; Jeftinija, S.; Lin, V. S. *J Am Chem Soc* **2003**, *125*, 4451.

(11) Stöber, W.; Fink, A.; Bohn, E. *J. Colloid Interface Sci.* **1968**, *26*, 62.

(12) Rao, K. S.; El-Hami, K.; Kodaki, T.; Matsushige, K.; Makino, K. *J. Colloid Interface Sci.* **2005**, *289*, 125.

(13) Rahman, I. A.; Vejayakumaran, P.; Sipaut, C. S.; Ismail, J.; Bakar, M. A.; Adnan, R.; Chee, C. K. *Colloids and Surfaces A: Physicochemical and Engineering Aspects* **2007**, *294*, 102.

(14) Won, J.; Cho, H.; Kang, Y. *Macromol. Res.* **2009**, *17*, 729.

(15) Ma, X.-k.; Lee, N.-H.; Oh, H.-J.; Kim, J.-W.; Rhee, C.-K.; Park, K.-S.; Kim, S.-J. *Colloids and Surfaces A: Physicochemical and Engineering Aspects* **2010**, *358*, 172.

(16) Cao, X. L.; Fischer, G. *Spectrochim Acta A* **1999**, *55*, 2329.

(17) Chuang, S.-W.; Hsu, S. L.-C.; Liu, Y.-H. *Journal of Membrane Science* **2007**, *305*, 353.

(18) Aslan, A.; Bozkurt, A. *Langmuir* **2010**, *26*, 13655.

(19) Nanjundan, S.; Unnithan, C. S.; Selvamalar, C. S. J.; Penlidis, A. *Reactive & Functional Polymers* **2005**, *62*, 11.

(20) Angell, C. L. *Journal of the Chemical Society (Resumed)* **1961**, 504.

(21) Aslan, A.; Bozkurt, A. *Solid State Ionics* **2013**, *239*, 21.